

Structural characterization and immunochemical detection of a fluorophore derived from 4-hydroxy-2-nonenal and lysine

LIN TSAI*[†], PAMELA A. SZWEDA^{†‡§}, OLGA VINOGRADOVA[‡], AND LUKE I. SZWEDA[‡]

*Laboratory of Biochemistry, National Heart, Lung, and Blood Institute, National Institutes of Health, Bethesda, MD 20892; [‡]Department of Physiology and Biophysics, School of Medicine, Case Western Reserve University, 10900 Euclid Avenue, Cleveland, OH 44106-4970

Communicated by E. R. Stadtman, National Heart, Lung and Blood Institute, Bethesda, MD, May 8, 1998 (received for review March 24, 1998)

ABSTRACT Aging and the progression of certain degenerative diseases are accompanied by increases in intracellular fluorescent material, termed “lipofuscin” and ceroid, respectively. These pigments are observed within granules composed, in part, of damaged protein and lipid. Modification of various biomolecules by aldehyde products of lipid peroxidation is believed to contribute to lipofuscin and ceroid formation. However, little direct evidence currently exists because the structures responsible for the fluorescent, cross-linked nature of this material are not well characterized. In this study, we have identified a fluorescent product formed in the reaction of N_{α} -acetyllysine and 4-hydroxy-2-nonenal (HNE), a major product of lipid peroxidation and the most reactive of these compounds under physiological conditions [Esterbauer, H., Shaur, R. J. & Zollner, H. (1991) *Free Radical Biol. Med.* 11, 81–128]. This fluorescent compound, characterized as a 2-hydroxy-3-imino-1,2-dihydropyrrrol derivative, appears to form upon oxidative cyclization of the nonfluorescent 2:1 lysine-HNE Michael adduct-Schiff base cross-link. Polyclonal antibody was raised to the N_{α} -acetyllysine-HNE fluorophore and found to be highly specific to the chromophore structure of the compound. This antibody has been used to conclusively demonstrate that the lysine-HNE derivative of this fluorophore forms on protein upon exposure to HNE. The results of this study therefore provide the basis for future investigations on the contribution(s) of HNE-derived fluorophore formation to lipofuscin and ceroid accumulation.

Aging and the progression of various degenerative diseases are accompanied by the accumulation of fluorescent pigments, lipofuscin and ceroid, within intracellular granules of postmitotic cells (for review, see 1–3). The histochemical and physical properties of lipofuscin and ceroid granules suggest that they are residual lysosomal bodies containing cross-linked aggregates of damaged cellular components (1–3). These pigments may therefore represent recognition and sequestration of damaged, nondegradable biomaterial by lysosomes. Although little direct evidence currently exists, it has been widely theorized that damage to cellular organelles by oxidative processes, in particular lipid peroxidation, contributes to lipofuscin and ceroid formation. This theory is based primarily on observations that incubation of various amine-containing compounds with lipid peroxidation products, such as malonaldehyde or 4-hydroxy-2-nonenal (HNE), results in the appearance of fluorescence reminiscent of lipofuscin and ceroid (excitation and emission maxima of 340–390 nm and 400–600 nm, respectively) (4–13). In addition, exposure of tissue homogenates to conditions which promote lipid peroxidation leads to increases in overall fluorescence (14–17).

The publication costs of this article were defrayed in part by page charge payment. This article must therefore be hereby marked “advertisement” in accordance with 18 U.S.C. §1734 solely to indicate this fact.

© 1998 by The National Academy of Sciences 0027-8424/98/957975-6\$2.00/0
PNAS is available online at <http://www.pnas.org>.

We have previously demonstrated that exposure of the model protein glucose-6-phosphate dehydrogenase (Glu-6-PDH) from *Leuconostoc mesenteroides* to HNE results in enzyme inactivation, mainly because of reaction of the ϵ -amino group of an active site lysine residue with the double bond (C3) of HNE forming a 1:1 lysine-HNE Michael adduct (18). Enzyme inactivation is followed by the appearance of cross-linked protein. Protein cross-linking results from reaction of the ϵ -amino group of two lysine residues with one molecule of HNE, one at the double bond (C3) and the other at the carbonyl group (C1) (19). In addition, cross-linking of protein by HNE is associated with the appearance of fluorescence (λ_{ex} = 340 nm, λ_{em} = 415 nm) reminiscent of lipofuscin and ceroid (9). Furthermore, we found that HNE cross-linked, fluorescent protein is resistant to proteolysis and acts as a potent noncompetitive inhibitor of the multicatalytic protease/proteasome, a proteolytic complex believed to be involved in the degradation of oxidatively modified forms of protein (9, 20). Thus, these observations suggest that modification of protein by HNE is involved in the age- and disease-related accumulation of oxidized protein, lipofuscin, and/or ceroid.

The goal of this study was to identify HNE-derived fluorophore(s) formed upon treatment of protein with HNE and to develop immunochemical methods for their detection. Based on results of previous experiments indicating the requirement for amino groups in fluorophore formation (4–14), we synthesized and characterized the structure of a fluorophore produced in the reaction of N_{α} -acetyllysine (NAL) with HNE. In addition, we prepared and immunopurified polyclonal antibody highly specific to the HNE-derived chromophore of the 2:1 NAL-HNE fluorophore (NAL₂HNE_f). As judged by immunochemical analysis, treatment of protein with HNE *in vitro* can lead to the formation of the fluorescent chromophore identified in model reactions. The results of this study therefore provide the basis for future investigations on the role of this fluorescent, HNE-derived protein modification in the accumulation of lipofuscin and ceroid during aging and the progression of certain diseases. While this work was in progress, we noted with interest the publication by Itakura *et al.* (21) on the structure of a fluorescent compound formed from the reaction of HNE with N_{α} -hippuryllysine. In addition, Xu and Sayre (22) proposed the analogous structure for a product from the reaction of 4-hydroxy-2-hexenal with *n*-butylamine.

MATERIALS AND METHODS

Materials. The following chemicals were purchased from commercial sources: NAL from Janssen; N_{α} -carbobenzoyloxy-

Abbreviations: NAL, N_{α} -acetyllysine; HNE, 4-hydroxy-2-nonenal; NAL₂HNE_f, structure **1a**; Glu-6-PDH, glucose-6-phosphate dehydrogenase; CA, carbonic anhydrase; TFA, trifluoroacetic acid; EDC, 1-ethyl-3-(3-dimethylaminopropyl)carbodiimide; KLH, keyhole limpet hemocyanin; MS, mass spectra.

[§]To whom reprint request should be addressed. e-mail: pas4@po.cwru.edu.

[†]L.T. and P.A.S. contributed equally to this work.

L-lysine from Sigma; 4-aminobutyric acid, ethyl 4-aminobutyrate hydrochloride, and ethylamine from Aldrich; 1-ethyl-3-(3-dimethylaminopropyl)carbodiimide (EDC) from Pierce. Glu-6-PDH from *L. mesenteroides* and carbonic anhydrase (CA) were obtained from Worthington. Keyhole limpet hemocyanin (KLH) was purchased from Pierce. I-Block for Western blot analyses was from Tropix (Bedford, MA).

HPLC. HPLC analyses were performed on a Hewlett-Packard model 1090 liquid chromatograph equipped with a Hewlett-Packard diode array UV detector and a Hewlett-Packard 1046A fluorescence detector.

Mass Spectral Analyses. Fast atom bombardment mass spectra were obtained from a JEOL SX-102 mass spectrometer operating at an accelerating voltage of 10 kV. Sample ions were desorbed from the matrix (magic bullet) by using six-ke xenon atoms.

NMR. NMR experiments were carried out using a Varian UNITYplus 600 MHz NMR spectrometer. A Varian 5 mm $^1\text{H}/\text{X}$ indirect z axis-pulsed field gradient probe was used. ^1H , ^{13}C , ^1H - ^{13}C heteronuclear single quantum coherence and ^1H - ^1H -correlated spectroscopy experiments were performed.

Preparation of 4-Hydroxy-2-nonenal (HNE). HNE dimethylacetal was synthesized as described (23). The dimethylacetal was hydrolyzed to HNE with 0.05% trifluoroacetic acid (TFA) in a 50% acetonitrile solution in water. HNE was purified by reverse-phase HPLC (Vydac C18 column, 1 ml/min, 0–50% acetonitrile vs. water, 0.05% TFA, in 0–20 min). The concentration of HNE was determined by absorbance at 224 nm by using $\epsilon_{224} = 13,750 \text{ M}^{-1}\text{cm}^{-1}$.

Reaction of HNE and NAL. Mixtures of HNE and NAL at various concentrations and pH values, and in the presence or absence of 100 μM Cu^{2+} , phosphate ion, and oxygen, were allowed to react at 37°C under agitation. Aliquots of the reaction mixture were withdrawn and analyzed by reverse-phase HPLC (Vydac C18 column, 1 ml/min, 0–50% acetonitrile vs. water, 0.05% TFA, in 0–20 min). Products were detected by UV absorbance at 210 and 360 nm. Fluorophore production was quantified by measuring the area of absorbance at 360 nm under the peak with a retention time of 13.9 min.

Preparation of the NAL-HNE Fluorophore (1a). NAL (4.7 g, 25 mmol) was dissolved in 25 ml of 0.2 M Na_2HPO_4 , pH 7.4. To this mixture was added a solution of HNE (75.5 mg/0.48 mmol, in 25 ml of water). The pH of the reaction mixture was adjusted to pH 7.4, and 50 μl of 100 mM CuSO_4 was added. The reaction was allowed to proceed at 37°C for 5 days with constant agitation. The reaction flask was exposed periodically to room air and the mixture vortexed to ensure the presence of oxygen. The fluorophore was isolated by three successive HPLC runs over a reverse-phase column (Vydac C18). The first purification step was accomplished by an acetonitrile-water (0.05% TFA) gradient (0–50% acetonitrile in 20 min). The subsequent two HPLC runs used a methanol-water (0.05% TFA) gradient (0–50% methanol in 20 min). The collected fractions were concentrated under a gentle stream of nitrogen and then lyophilized to yield a light yellow solid, 10.0 mg (0.02 mmol, 4.1% yield based on HNE). Fast atom bombardment/mass spectra (MS): MH^+ 511. HR-MS: Observed 511.3128. Calculated for $\text{C}_{25}\text{H}_{43}\text{O}_7\text{N}_4$: 511.3132. UV: λ_{max} (H_2O , pH 7) 360 nm; $\epsilon_{360} = 11,250 \text{ M}^{-1}\text{cm}^{-1}$. Fluorescence: $\lambda_{\text{ex}} = 360 \text{ nm}$, $\lambda_{\text{em}} = 430 \text{ nm}$. ^{13}C -NMR (150 MHz; CD_3OD as 49.0 ppm; number of carbon atoms are given in parenthesis): δ (ppm): 14.206 (1), 22.396 (2), 22.882 (1), 23.989 (2), 28.934 (1), 29.626 (1), 32.316 (2), 37.155 (1), 45.269 (1), 46.513 (1), 53.202 (2), 88.907 (1), 97.143 (1), 167.704 (1), 173.377 (2), 175.227 (2), and 179.186 (1). ^1H -NMR (600 MHz; CD_3OD as 3.35 ppm): δ (ppm): 0.87 (^3H , t), 0.94 (2H, m), 1.3 (4H, m), 1.45 (4H, m), 1.7–1.9 (9H, m), 2.0 (6H, s), 2.1 (1H, m), 3.4 (2H, m), 3.5 (2H, m), 4.4 (1H, m), 5.5 (1H, d), 8.300 (1/2H, d), and 8.305 (1/2H, d).

General Procedure for the Reaction of HNE with Primary Amines. An amino compound (1.65 mmol) was dissolved in 10 ml of 0.2 M Na_2HPO_4 buffer containing 100 μM CuSO_4 . The pH was adjusted to 7.2. To this mixture was added HNE (0.165 mmol) in 2.5 ml of acetonitrile. The reaction mixture was stirred in a 37°C water bath for 5–20 days. The progress of the reaction was monitored by HPLC analysis at intervals. At optimal production of fluorophore, the reaction was stopped by acidification with TFA. The mixture was evaporated in a rotoevaporator at 37°C under reduced pressure. The resulting syrupy residue was triturated repeatedly with ethanol, which dissolved the fluorophore. The precipitated salts were removed by filtration. The combined ethanol filtrates were purified by HPLC. The fluorophore was collected and analyzed by fast atom bombardment/MS. The results are tabulated in Table 2. These compounds all exhibited $\lambda_{\text{ex}}/\lambda_{\text{em}}$ at 360/430 nm.

Incubation of Protein with HNE. Glu-6-PDH from *L. mesenteroides* or CA was suspended in 50 M K_2HPO_4 and 200 mM KCl (pH 7.4) by passage through a PD-10 column (Pharmacia) previously equilibrated with the buffer. The reaction was initiated by addition of 10 mM HNE to an equal volume of protein (5.0 mg/ml) in 50 mM K_2HPO_4 and 200 mM KCl (pH 7.4) and allowed to proceed at 37°C. After 0, 0.5, 1.0, 2.0, and 4.0 h, an aliquot of the reaction mixture was treated with 5.0 mM NaBH_4 in 0.1 M NaOH for 5 min to stabilize the nonfluorescent 2:1 amino acid-HNE protein cross-links as previously described (9, 19). We have determined that the 2:1 lysine-HNE fluorophore is not reduced under these conditions (not shown). After neutralization with 1 M HCl, the protein solution was passed over a PD-10 column with 100 mM Na_2HPO_4 (pH 7.4) as eluant.

Preparation of Polyclonal Antibody to NAL_2HNE_f (1a). Fluorophore-linked KLH was prepared by reacting 2.0 mg KLH, 3.5 mg NAL_2HNE_f (1a) (6.9 μmol), and 0.5 mg EDC (2.6 μmol) in 750 μl of 0.1 M Mes and 0.9 M NaCl (pH 4.7). After 2 h at 25°C, unreacted NAL_2HNE_f (1a) and reaction byproducts were removed by gel filtration over a PD-10 column with 0.083 M Na_2HPO_4 and 0.9 M NaCl, stabilizers (pH 7.2) (Pierce) as eluant.

Immunization Protocol. Polyclonal antibody was generated in New Zealand White female rabbits. To initiate the immunization protocol, a 0.5 ml aliquot of fluorophore-linked KLH (1.0 mg/ml) was diluted with an equal volume of Freund's incomplete adjuvant and injected into the rabbit (intradermal back). Thereafter, booster injections (125–250 μg of immunogen diluted in Freund's incomplete adjuvant, s.c. dorsal) were made every 21 days. Test bleeds were obtained 10 days after each inoculation and antibody titer was monitored by ELISA.

Immunopurification of Polyclonal Antibody. An affinity column was prepared by covalent attachment of NAL_2HNE_f (1a) to agarose-immobilized diaminodipropylamine (Pierce) via EDC coupling. Briefly, 0.15 mg (0.29 μmol) of NAL_2HNE_f ($\epsilon_{360} = 11,250 \text{ M}^{-1}\text{cm}^{-1}$) was dissolved in 3.0 ml of 0.1 M Mes (pH 4.7). The NAL_2HNE_f solution was incubated with 2.0 ml of 50% agarose-immobilized diaminodipropylamine slurry (Pierce) for 2 h (25°C), and the affinity column washed with 10 mM Na_2HPO_4 , 100 mM KCl (pH 7.4), and 100 mM glycine (pH 2.8). After equilibration of the column with 10 mM Na_2HPO_4 and 100 mM KCl (pH 7.4), 0.9 ml of antisera was mixed with 1.8 ml of the same buffer, applied to the column, and incubated at 25°C for 1 h 15 min. The column was washed extensively with 10 mM Na_2HPO_4 and 100 mM KCl (pH 7.4) followed by elution of anti- NAL_2HNE_f by using 100 mM glycine (pH 2.8). The pH of the antibody solution was adjusted to 7.4 by adding an appropriate volume of 1.0 M Tris, pH 8.0. Before use, an equal volume of glycerol was added to the antibody solution. As determined by using the bicinchoinic acid protein assay with BSA as standard, 2.8 mg of

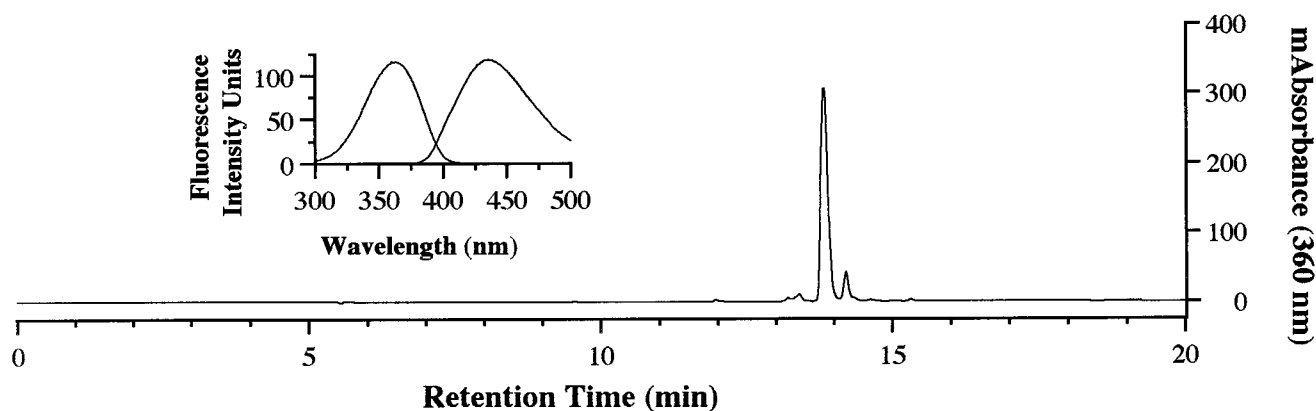


FIG. 1. HPLC resolution of products formed in the reaction of NAL and HNE. NAL (94.0 mg) was reacted with HNE (1.56 mg) in 0.1 M Na_2HPO_4 , pH 7.4 ($V_{\text{run}} = 1.0$ ml) for 20 h at 37°C. A 25 μl aliquot of the reaction mixture was analyzed by reverse-phase HPLC by using a Vydac C18 column (*Materials and Methods*). The elution profile was obtained by monitoring absorbance at 360 nm. (*Inset*) The major 360 nm-absorbing peak was collected and the fluorescence spectrum obtained by using a Shimadzu RF-5301 spectrofluorimeter ($\lambda_{\text{ex}} = 360$ nm, $\lambda_{\text{em}} = 430$ nm).

immunopurified antibody is typically obtained from 0.9 ml of antisera.

Antibody Characterization by ELISA. Coating antigen was prepared by covalently linking NAL_2HNE_f (**1a**) to CA via EDC coupling. Typically, 0.4 mg of NAL_2HNE_f (0.8 μmol) in 100 μl of water was mixed with 0.88 mg of CA in 0.5 ml of 20 mM Na_2HPO_4 and 0.1 M NaCl (pH 7.2). To this solution was added 0.15 mg (0.8 μmol) of EDC-HCl. The reaction was allowed to proceed for 2 h at 25°C. The NAL_2HNE_f -linked CA was passed over a PD-10 column with the same buffer as eluant. The degree of fluorophore incorporation was determined after HPLC purification of NAL_2HNE_f -linked CA (Vydac C18 column, 0–50% acetonitrile vs. water, 0.05% TFA, in 20 min). Protein concentration was determined by using the bicinchoninic acid assay with BSA as standard. Fluorophore content was estimated by comparing the intensity of signal at 360 nm with a standard curve constructed by using known quantities of NAL_2HNE_f (**1a**). In general, under the conditions of our coupling reactions, ≈ 2.5 nmol of fluorophore was linked to 1.0 mg of carbonic anhydrase.

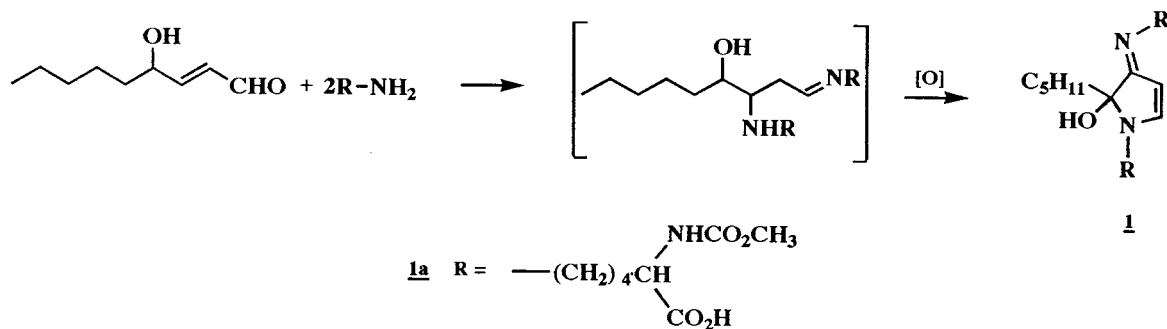
In a typical ELISA, an aliquot of coating antigen solution was diluted into 0.2 M $\text{NaHCO}_3/\text{Na}_2\text{CO}_3$ buffer, pH 9.4 and applied to a microtiter plate. After 1 h at 25°C, the wells were rinsed with 3×100 μl of PBS containing 0.05% Tween-20 and 0.1% BSA (wash buffer) and blocked (1% BSA in PBS) for 1 h (25°C). A 100 μl aliquot of anti- NAL_2HNE_f antibody (28 $\mu\text{g}/\text{ml}$ in blocking buffer) was applied to the wells and incubated for 1 h (25°C). In competition studies, varying concentrations of competitors were added to the wells before addition of primary antibody. The wells were then rinsed with 3×100 μl of wash buffer and incubated in 100 μl goat anti-rabbit IgG conjugated to alkaline phosphatase (Pierce, 1:7500 in blocking buffer) for 1 h (25°C). After 3×100 μl rinses with wash buffer and 2×100 μl rinses with 20 mM

Tris-Base, pH 9.8, containing 1 mM MgCl_2 (assay buffer), a 100- μl aliquot of 1 mg/ml *p*-nitrophenyl phosphate (PNPP, Pierce in assay buffer) were added. The microtiter plate was then read in a Bio-Rad model 500 microplate reader (405 nm) in the kinetic mode (30 min at 25°C). Typically, two readings/min were taken. Relative rates of *p*-nitrophenyl phosphate hydrolysis, within the linear range, were then used to evaluate primary antibody binding.

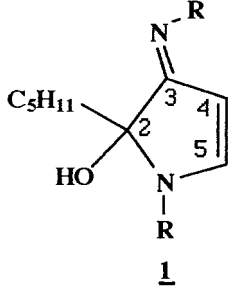
Western Blot Analysis. Samples were subjected to SDS/PAGE and Western blot analysis. Briefly, 2.0 $\mu\text{g}/\text{lane}$ of protein solution was applied to a series of two 10% polyacrylamide gels. One gel was stained with Coomassie blue to visualize the protein distribution. The other gel was used to electroblot proteins onto a nitrocellulose membrane (0.45 μm). Membrane-immobilized proteins were incubated with anti- NAL_2HNE_f diluted 1:2000 into blocking buffer (0.2% I-block in PBS containing 0.1% Tween-20) overnight at 25°C. After 3×10 -min washes with PBS containing 0.1% Tween-20 (wash buffer), the membrane was incubated with goat anti-rabbit IgG conjugated to alkaline phosphatase (Tropix, diluted 1:10,000 in blocking buffer) for 1 h at 25°C. The membrane was then rinsed 3×5 min with wash buffer and 2×5 min with assay buffer (20 mM Tris base, pH 9.8, containing 1 mM MgCl_2). After incubation with a chemiluminescent alkaline phosphatase substrate (1.25 mM CSPD and 1 mg/ml Nitro-Block from Tropix in assay buffer), antibody binding was visualized by autoradiography.

RESULTS AND DISCUSSION

Formation of Fluorophore from NAL and HNE. Reaction of NAL (0.5 M) with HNE (10 mM) in Na_2HPO_4 (0.1 M, pH 7.4) at 37°C for 20 h resulted in the formation of a compound which could be resolved by reverse-phase HPLC (Fig. 1) and exhib-

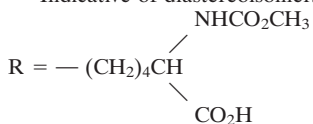


Scheme. Formation of N_α -acetyllysine-HNE fluorophore.

Table 1. Assignment of selected ^1H and ^{13}C resonances


Assignments	δ_c , ppm	δ_h , ppm
C-2	97.143	
C-3	179.186	
C-4	88.907	5.5 (d)
C-5	167.704	8.300 (d)* 8.305 (d)*
NCOCH ₃	173.377	
NCOCH ₃	22.396	2.0 (s)
CO-OH	175.227	
=N-CH ₂	46.510	3.5 (m)
N-CH ₂	45.270	3.4 (m)
NH-CH-CO ₂ H	53.202	4.4 (m)

*Indicative of diastereoisomers

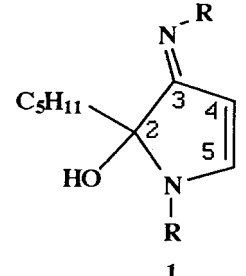


ited a UV absorbance maximum of 360 nm. This compound was fluorescent, with excitation and emission maxima at 360 and 430 nm, respectively (Fig. 1, *Inset*). To characterize this fluorophore and develop methods for its detection in biological samples, it was desirable to optimize the conditions of its formation. We therefore determined the effects of relative concentrations of HNE and NAL, pH, and the presence or absence of Cu^{2+} , phosphate, and oxygen on fluorophore yield (not shown). These experiments indicated that formation of

the fluorophore required a large excess of NAL to HNE (50:1 in these studies) and the presence of phosphate (optimal pH of 7.4) and oxygen. In addition, the reaction was catalyzed by Cu^{2+} (100 μM), suggesting the involvement of oxidative events in fluorophore production. Thus, the preparation of a small amount of this fluorophore was archived (*Materials and Methods*). Analysis by fast atom bombardment/MS gave a quasi-molecular ion of 511 (MH^+), suggesting that the fluorophore was derived from one molecule of HNE and two molecules of NAL. High resolution mass measurement generated an empirical formula of $\text{C}_{25}\text{H}_{42}\text{N}_4\text{O}_7$ (*Materials and Methods*). This formula is four hydrogen atoms less than that of the 2:1 NAL-HNE Michael-Schiff base adduct ($\text{C}_{25}\text{H}_{46}\text{N}_4\text{O}_7$), indicating an oxidative process in its formation. The molar absorptivity of the fluorophore was estimated to be 11,250 $\text{M}^{-1}\text{cm}^{-1}$ at 360 nm from measurements of mass and UV absorbance (aqueous solutions, pH 7.0). The ^1H and ^{13}C NMR spectra (Table 1) are consistent with structure **1a** (Scheme), a 2-hydroxy-3-imino-1,2-dihydropyrrol derivative, as proposed by Itakura *et al.* (21) as well as by Xu and Sayre (22) for similar compounds. We have demonstrated the general nature of this reaction by observation of the formation of analogous fluorophores from the reaction of HNE with a number of primary amines (Table 2). All these compounds show the 360/430-nm excitation/emission maxima. Their polar nature is reflected by their solubility in water or methanol. They are stable at slightly acidic pH, presumably due to protonation of the Schiff base nitrogen. Under alkaline conditions (pH \geq 9.0), they decompose upon standing, as shown by the gradual disappearance of fluorescence. However no discrete degradation products have yet been identified.

Antibody Sensitivity and Specificity. Polyclonal antibody was raised to NAL_2HNE_f -linked KLH. After immunopurification (*Materials and Methods*), the binding properties of anti- NAL_2HNE_f were characterized by ELISA. Under the conditions described in *Materials and Methods*, the antibody could readily detect as little as 15 fmol of fluorophore (not shown). As judged by competitive ELISA with NAL_2HNE_f -linked CA as coating antigen (1.0 pmol NAL_2HNE_f /well), antibody binding was competed by NAL_2HNE_f (IC_{50} of \approx 0.1 μM) but not by 1:1 N_α -acetylhistidine- and N_α -acetylcysteine-

Table 2. Mass spectral data for amine-HNE fluorophores



	R	Observed MH^+	Calculated MH^+	Formula
1a	NHCOCH ₃	511.3128	511.3132	$\text{C}_{25}\text{H}_{43}\text{O}_7\text{N}_4$
	$\begin{array}{l} \text{---}(\text{CH}_2)_4\text{CH} \\ \\ \text{CO}_2\text{H} \end{array}$			
1b	NHCO ₂ CH ₂ C ₆ H ₅	695.3687	695.3690	$\text{C}_{37}\text{H}_{51}\text{O}_9\text{N}_4$
	$\begin{array}{l} \text{---}(\text{CH}_2)_4\text{CH} \\ \\ \text{CO}_2\text{H} \end{array}$			
1c	$\text{---}(\text{CH}_2)_3\text{CO}_2\text{H}$	341.2065	341.2076	$\text{C}_{17}\text{H}_{20}\text{O}_5\text{N}_2$
1d	$\text{---}(\text{CH}_2)_3\text{CO}_2\text{C}_2\text{H}_5$	397.2694	397.2703	$\text{C}_{21}\text{H}_{37}\text{O}_5\text{N}_2$
1e	$\text{---CH}_2\text{CH}_3$	225.1967	225.1967	$\text{C}_{13}\text{H}_{25}\text{O}_5\text{N}_2$

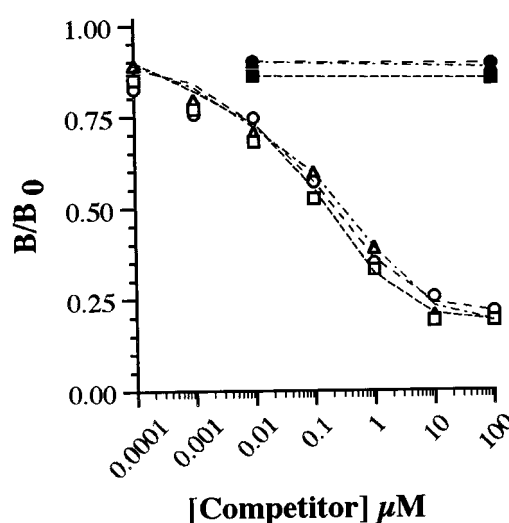
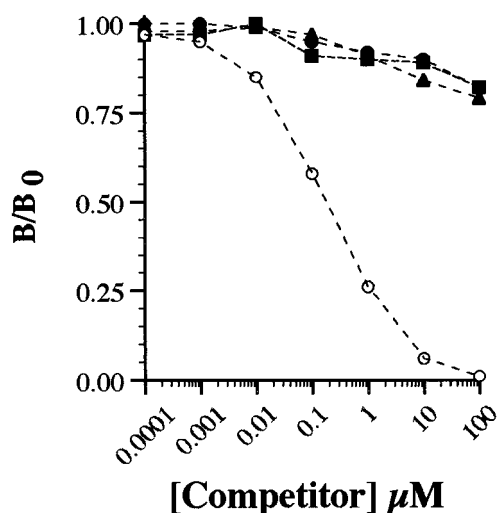


FIG. 2. Specificity of polyclonal antibody raised to NAL₂HNE_f (**1a**). As detailed in *Materials and Methods*, competitive ELISA was performed by using immunopurified anti-NAL₂HNE_f as primary antibody and NAL₂HNE_f-linked CA (1.0 pmol NAL₂HNE_f/well) as coating antigen. Antibody binding was evaluated in the presence of NAL₂HNE_f (○) and adducts produced in the reactions of HNE with N α -acetylhistidine (▲), N α -acetylcysteine (■), and NAL (●), at concentrations indicated on the *abscissa*. $B/B_0 = [(OD/s) - (OD/s)_{\text{bkg}}] / [(OD/s)_{\text{no competitor}} - (OD/s)_{\text{bkg}}]$ where OD/s = change in absorbance at 405 nm per s in the linear range. Background (bkg) values were obtained by using CA exposed to EDC in the absence of NAL₂HNE_f (**1a**) as coating antigen (*Materials and Methods*).

FIG. 3. Binding of anti-NAL₂HNE_f to HNE-treated Glu-6-PDH. As detailed in *Materials and Methods*, the binding of immunopurified anti-NAL₂HNE_f to Glu-6-PDH-linked Lys-HNE fluorophore (60 fmol/well) was evaluated by ELISA. In addition, antibody binding was evaluated in the presence of NAL₂HNE_f (**1a**) (○), fluorophores produced in the reactions of HNE with γ -aminobutyric acid (**1c**) (□) and ethylamine (**1e**) (▲), and nonderivitized NAL (●), γ -aminobutyric acid (■), and ethylamine (▲). $B/B_0 = [(OD/s) - (OD/s)_{\text{bkg}}] / [(OD/s)_{\text{no competitor}} - (OD/s)_{\text{bkg}}]$ where OD/s = change in absorbance at 405 nm/s in the linear range. Background (bkg) values were obtained by using Glu-6-PDH treated with HNE for 0 min (*Materials and Methods*).

HNE Michael adducts or 1:1 and 2:1 NAL-HNE adducts at concentrations $\leq 100 \mu\text{M}$ (Fig. 2). It should be noted that, for nonfluorescent NAL-HNE adducts, competition studies were performed with a mixture of 1:1 and 2:1 derivatives (combined concentrations as indicated in Fig. 2) because these adducts are not readily resolved by HPLC. Furthermore, NAL₂HNE_f-linked CA was not recognized by antibody raised to 1:1 amino acid-HNE Michael adducts (24). As an additional test of antibody specificity, HNE-treated CA was evaluated by ELISA and Western blot analyses. Exposure of CA to HNE does not result in the formation of cross-linked protein or the appearance of protein-associated fluorescence (not shown). Consistent with these observations, HNE-treated CA was not recognized by anti-NAL₂HNE_f (not shown) but was recognized by antibody raised to 1:1 amino acid-HNE Michael adducts (24). Thus, immunopurified polyclonal antibody is specific to

NAL₂HNE_f (**1a**) and, under the conditions of these experiments, displays a sensitivity in the femtomol range.

Formation of the Fluorophore on Protein. We had previously found that treatment of Glu-6-PDH from *L. mesenteroides* with HNE for extended periods of time led to the appearance of fluorescent, cross-linked protein (9). In this study, we have determined that HNE-induced fluorescence was due, at least in part, to formation of structure **1** (R = lysine residues). To induce formation of cross-links and fluorophore(s), Glu-6-PDH (2.5 mg/ml) was treated with HNE (5.0 mM) at 37°C. At various time points, HNE Michael adducts and nonfluorescent cross-links were reductively stabilized by reaction with NaBH₄ as described (*Materials and Methods*). These mild conditions (5.0 mM NaBH₄/0.1 mM NaOH, pH 7.5–8.0; 5 min at 25°C) do not result in reduction or decomposition of NAL₂HNE_f (**1a**) or abolish Glu-6-PDH-associated fluorescence. As judged by ELISA (Fig. 3), Glu-6-PDH incu-

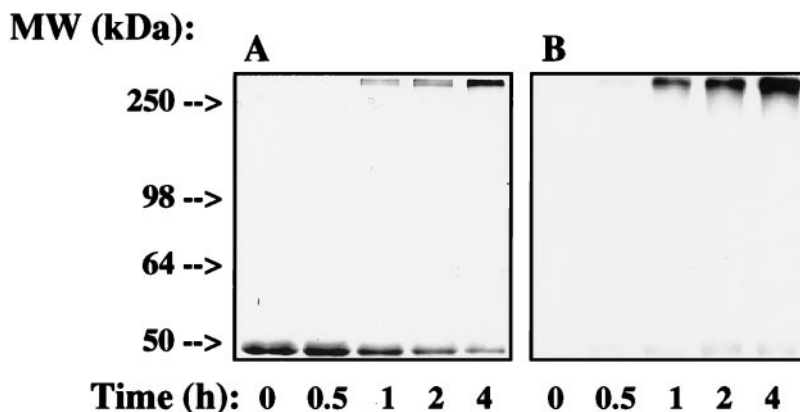


FIG. 4. SDS-PAGE and Western blot analysis of Glu-6-PDH treated with HNE. Glu-6-PDH (2.5 mg/ml) was incubated with HNE (5.0 mM) for 0, 0.5, 1.0, 2.0, and 4.0 h at 37°C as detailed in *Materials and Methods*. Samples were loaded onto two 10% polyacrylamide gels (2.0 μg /well). One gel of the series was stained with Coomassie blue for evaluation of the molecular weight distribution of HNE-treated Glu-6-PDH (A). The other gel was electroblotted onto nitrocellulose membrane (0.45 μm) for Western blot analysis with immunopurified anti-NAL₂HNE_f (1/2,000) as primary antibody (B). Antibody binding was visualized after exposure of the blot to a chemiluminescent substrate (*Materials and Methods*).

bated with HNE for 4.0 h (37°C) was recognized by immunopurified anti-NAL₂HNE_f, suggesting that HNE-induced protein fluorescence (9) is due to formation of the lysine-HNE fluorophore **1** (R = lysine residues). The level of antibody binding corresponded to ≈0.15 nmol of lysine-HNE fluorophore per milligram of protein relative to an ELISA standard curve constructed by using known amounts of NAL₂HNE_f/well (as NAL₂HNE_f-linked CA). To obtain further evidence that the HNE-derived fluorophore on HNE-treated Glu-6-PDH was identical to that identified in the model reaction between NAL and HNE, competitive ELISA with HNE-treated Glu-6-PDH as coating antigen was performed. As shown in Fig. 3, antibody binding could be competed by NAL₂HNE_f and by analogous fluorophores produced by reaction of γ -aminobutyric acid and ethylamine with HNE (Table 2). The kinetics of competition were identical, with the IC₅₀ for antibody binding being ≈0.1 μ M for each fluorophore tested. These observations demonstrate that the epitope recognized by the antibody is the 2-hydroxy-3-imino-1,2-dihydropyrrrol structural feature (**1**, Scheme) of fluorophores produced by reaction of primary amines with HNE (Table 2) and that this structure (**1**, R = lysine residues) forms when Glu-6-PDH is exposed to HNE. To evaluate the distribution of fluorophore-modified Glu-6-PDH as a function of time of exposure to HNE, Glu-6-PDH treated with HNE for 0, 0.5, 1.0, 2.0, and 4.0 h was analyzed by SDS/PAGE and Western blot analysis. As shown in Fig. 4A, this resulted in the formation of cross-linked, multimeric protein, the relative levels of which increased in a time-dependent fashion. Di- and tetrameric forms of Glu-6-PDH, visible in the gel but not readily seen in Fig. 4A, were converted rapidly to aggregated protein under the conditions of our experiments. Increases in the level of multimeric protein were paralleled by increases in the intensity of protein-associated fluorescence (not shown) (9) and in the level of anti-NAL₂HNE_f binding (Fig. 4B). The distribution of antibody binding indicated that fluorescent, lysine-HNE cross-links (**1**, R = lysine residues) were present primarily on multimeric protein (Fig. 4B). This observation suggests that fluorescent cross-links represent relatively stable end products of HNE modification(s). However, some binding to monomeric protein was evident, indicating the presence of relatively low levels of intramolecular lysine-HNE fluorescent cross-links (**1**, R = lysine residues). Thus, these results provide strong evidence that the HNE-derived fluorophore **1** (R = lysine residues) is produced when Glu-6-PDH is incubated with HNE *in vitro*.

In summary, the HNE-derived fluorophore (**1a**) obtained in the model reaction of NAL and HNE appears to be an oxidative cyclized product of the previously described 2:1 lysine-HNE Michael adduct-Schiff base cross-link (Scheme) (19). Based on spectroscopic data (*Materials and Methods*), the proposed structure (**1a**) is consistent with that reported by Itakura *et al.* (21) and Xu and Sayre (22) for fluorophores derived from *N*_α-hippuryllysine and HNE and from *n*-butylamine and 4-hydroxy-2-hexenal, respectively. Polyclonal antibody generated to NAL₂HNE_f (**1a**) covalently linked to KLH was found to recognize the 2-hydroxy-3-imino-1,2-dihydropyrrrol nucleus of **1** (Table 2, Figs. 2 and 3). As shown in Figs. 3 and 4, we have used this antibody to demonstrate conclusively that treatment of Glu-6-PDH (2.5 mg/ml) with HNE (5.0 mM) results in the production of the lysine-HNE fluorophore **1** (R = lysine residues, 0.15 nmol/mg protein after 4.0 h at 37°C). It should be noted that the fluorescence properties of HNE cross-linked Glu-6-PDH ($\lambda_{\text{ex}} = 340$ nm, $\lambda_{\text{em}} = 415$ nm) (9) differ from those of NAL₂HNE_f ($\lambda_{\text{ex}} = 360$ nm, $\lambda_{\text{em}} = 430$ nm). This may reflect the presence of other as yet unidentified HNE-derived fluorophores on the protein or changes in fluorescence properties due to protein structure. Thus, experiments seeking direct chemical evidence for the

2-hydroxy-3-imino-1,2-dihydropyrrrol nucleus of **1** (R = lysine residues) on HNE-modified fluorescent protein are currently underway in this laboratory.

Accumulation of fluorescent, cross-linked protein aggregates within intracellular granules has been associated with aging (lipofuscin) and with the progression of various degenerative diseases (ceroid) (1–3). Although it has been suggested that the formation of these pigments is due, in part, to modification of proteins by lipid peroxidation products, little direct evidence is currently available. We have previously shown that HNE cross-linked, fluorescent protein is resistant to proteolysis and acts as a potent inhibitor of the multicatalytic protease/proteasome, an enzyme complex involved in the degradation of oxidatively modified protein (9, 20). Thus, HNE modifications to protein may contribute to the accumulation of damaged forms of protein as a function of age and disease state. The results of this study and the methods developed are therefore critical to future investigations aimed at elucidating: (i) The relative contribution of HNE-derived fluorophores to lipofuscin and ceroid accumulation *in vivo*; (ii) the subcellular origin(s) of damaged cellular components present in these heterogeneous, fluorescent pigments; (iii) the effects of protein cross-linking and fluorophore formation on specific physiological functions; and (iv) mechanisms by which cells respond to free radical and lipid peroxidation damage.

This work was supported by a Scientist Development grant from the American Heart Association (9630025N) and with funds contributed in part by the American Heart Association, Northeast Ohio Affiliate. We thank Dr. Lewis Pannell, Laboratory of Analytical Chemistry, National Institute of Diabetes and Digestive and Kidney Disease, National Institutes of Health for performing mass-spectroscopic determinations.

1. Harman, D. (1990) in *Lipofuscin and Ceroid Pigments*, ed. Porta, E. A. (Plenum, New York), pp. 3–15.
2. Porta, E. A. (1991) *Arch. Gerontol. Geriatr.* **12**, 303–320.
3. Yin, D. (1996) *Free Radical Biol. Med.* **21**, 871–888.
4. Chio, K. S. & Tappel, A. L. (1969) *Biochemistry* **8**, 2821–2827.
5. Chio, K. S. & Tappel, A. L. (1969) *Biochemistry* **8**, 2827–2833.
6. Dillard, C. J. & Tappel, A. L. (1971) *Lipids* **6**, 715–721.
7. Kikugawa, K. & Beppu, M. (1987) *Chem. Phys. Lipids* **44**, 277–296.
8. Nair, V., Offerman, R. J., Turner, G. A. & Pryor, A. N. (1988) *Tetrahedron* **44**, 2793–2803.
9. Friguet, B., Stadtman, E. R. & Szweda, L. I. (1994) *J. Biol. Chem.* **269**, 21639–21643.
10. d'Ischia, M., Costantini, C. & Prota, G. (1996) *Biochim. Biophys. Acta* **1290**, 319–326.
11. Chen, P., Wiesler, D., Chmelik, J. & Novotny, M. (1996) *Chem. Res. Toxicol.* **9**, 970–979.
12. Uchida, K., Sakai, K., Tiakura, K., Osawa, T. & Toyokuni, S. (1997) *Arch. Biochem. Biophys.* **346**, 45–52.
13. Zidek, L., Doleze, P., Chmelik, J., Baker, A. G. & Novotny, M. (1997) *Chem. Res. Toxicol.* **10**, 702–710.
14. Tsuchida, M., Miura, T., Mizutani, K. & Aibara, K. (1985) *Biochim. Biophys. Acta* **834**, 196–204.
15. Esterbauer, H., Koller, E., Snee, R. G. & Koster, J. F. (1986) *Biochem. J.* **239**, 405–409.
16. Hoff, H. F., Whitaker, T. E. & O'Neil, J. (1992) *J. Biol. Chem.* **267**, 602–609.
17. Nilsson, E. & Yin, D. (1997) *Mech. Ageing Dev.* **99**, 61–78.
18. Szweda, L. I., Uchida, K., Tsai, L. & Stadtman, E. R. (1993) *J. Biol. Chem.* **268**, 3342–3347.
19. Cohn, J. A., Tsai, L., Friguet, B. & Szweda, L. I. (1996) *Arch. Biochem. Biophys.* **328**, 158–164.
20. Friguet, B. & Szweda, L. I. (1997) *FEBS Lett.* **405**, 21–25.
21. Itakura, K., Osawa, T. & Uchida, K. (1998) *J. Org. Chem.* **63**, 185–187.
22. Xu, G. & Sayre, L. M. (1998) *Chem. Res. Toxicol.* **11**, 247–251.
23. De Montarby, L., Tourbah, H. & Gree, R. (1989) *Bull. Soc. Chim. Fr.* **3**, 419–431.
24. Uchida, K., Szweda, L. I., Chae, H.-Z. & Stadtman, E. R. (1993) *Proc. Natl. Acad. Sci. USA* **90**, 8742–8746.